The concept of joint saturation and its application

Yunhui Tan, Thomas Johnston, and Terry Engelder

ABSTRACT

Two of the major joint-driving mechanisms are joint-normal stretching and poroelastic shrinkage, and these lead to joint sets commonly associated with structural bending and natural hydraulic fracturing, respectively. Regardless of joint-driving mechanism, joint infilling is a nonhomogeneous Poisson process in the presence of stress shadows. Through probability modeling, we show that in all cases joint spacing is best fit with gamma distributions. The shape parameter of the best-fit gamma distribution to joint-spacing data is a quantitative means to assess the extent of saturation, which is represented in a new parameter, the joint-saturation ratio (JSR). To test the utility of JSR, we call upon published structural bending joint data (Elk Basin, Lilstock, and Rives plate-bending experiment). The shape parameters for these well-developed structural bending joints are equal to around three, corresponding to a JSR of approximately 30%. Using the same analysis on the spacing of natural hydraulic fractures collected from outcrops in the gas-prone Devonian sections of the Appalachian Basin, we find that natural hydraulic fractures differ in two aspects from structural bending joints. First, the joint spacing is proportional to bed thickness in bedded rocks but not in gas shale sections. Second, the joint saturation of natural hydraulic fractures is generally lower than in well-developed structural bending joints. Thus, the JSR is a means to distinguish the joint-driving mechanism and to represent joint-saturation level independent of bed thickness effects. It can be used to distinguish natural fractures from drilling-induced fractures and to improve the fracture-network modeling.

INTRODUCTION

Joint-Driving Mechanisms

Two major joint-driving mechanisms are joint-normal stretching and poroelastic shrinkage (Engelder and Fischer, 1996). These

Manuscript received June 28, 2013; provisional acceptance January 16, 2014; revised manuscript received April 16, 2014; final acceptance June 23, 2014.
DOI: 10.1306/06231413113

AUTHORS

YUNHUI TAN ~ *Pennsylvania State University, Department of Geosciences, University Park, Pennsylvania, 16802; tanyunhui@gmail.com*

Yunhui Tan received his B.E. degree in resource prospecting engineering (petroleum geology) from China University of Petroleum (East China) in 2010. He is currently pursuing a Ph.D. in geosciences at Pennsylvania State University with Terry Engelder. His thesis is on the fractures in the Appalachian Basin and microseismic monitoring of hydraulic fracturing. He is also interested in geomechanics.

THOMAS JOHNSTON ~ *Pennsylvania State University, Department of Geosciences, University Park, Pennsylvania, 16802; tjj2g08@gmail.com*

Thomas Johnston received an M.Sci. degree in geology from the University of Southampton, United Kingdom in 2012. During his year of study abroad in 2011, he completed fieldwork with Yunhui Tan and Terry Engelder. He is currently completing his M.S. degree in geology at Pennsylvania State University with Terry Engelder. His thesis focuses on in situ stress measurements and geomechanical modeling of the Marcellus Shale.

TERRY ENGELDER ~ *Pennsylvania State University, Department of Geosciences, University Park, Pennsylvania, 16802; jte2@psu.edu*

Terry Engelder, a leading authority on the Marcellus gas shale play, received his B.S. degree from Pennsylvania State University (1968), his M.S. degree from Yale University (1972), and his Ph.D. from Texas A&M University (1973). He is currently a professor of geosciences at Pennsylvania State University and has previously served on the staff of the U.S. Geological Survey, Texaco, and Lamont-Doherty Earth Observatory. He has written 160 research papers, many focused on fracture in Devonian rocks of the Appalachian Basin, and a book, *Stress Regimes in the Lithosphere*.

ACKNOWLEDGEMENTS

We thank Guolong Su for discussions on statistics and stochastic processes. Helpful reviews by Taixu Bai, Peter Hennings, David Haddad, and Alan Morris, together with the editorial comments from David Ferrill and Michael Sweet, helped us improve the manuscript. We would also like to thank Haiqing Wu for many insightful comments and discussions. This project was supported by RPSEA-GTI Project 9122-04 and by the Pennsylvania State Appalachian Basin Black Shale Group.

The AAPG Editor and the special issue editor David A. Ferrill thank the following reviewers for their work on this paper: Taixu Bai, David E. Haddad, Peter Hennings, and Alan P. Morris.

driving mechanisms lead to joint sets characteristic of structural bending and natural hydraulic fracturing, respectively. Structural bending is commonly most severe near the hinges of folds where extensional strain, coupled with hydrostatic pore pressure, causes a relaxation in effective compressional stress to the extent that joints grow in the stiffer layers of a well-bedded clastic or carbonate rock. In the oil and gas industry, it is widely accepted that these joints can be modeled using curvature attributes from reflection seismic data (Chopra and Marfurt, 2007) or three-dimensional (3-D) structural models (Hennings et al., 2000; McLennan et al., 2009).

In the absence of structural bending, natural hydraulic fracturing may well be the most common joint type in clastic basins where source rocks are common (Lash and Engelder, 2011). Natural hydraulic fracturing as a joint-driving mechanism in the subsurface was first proposed by Secor (Secor, 1965). Secor combined Griffith theory of failure with effective stress and concluded that tension fractures could be formed at significant depth in the basin as long as the fluid pressure approaches that of the overburden. Other authors further simulated natural hydraulic fracturing in basins and looked at its relationship with hydrocarbon maturation (Palciauskas and Domenico, 1980; Ungerer et al., 1990).

Natural hydraulic fracturing occurs when the strain caused by the poroelastic deformation of the matrix from overpressured pore fluid leads to a crack-tip stress intensity that exceeds the fracture toughness of the rock (Engelder and Lacazette, 1990). Miller (1995) made the distinction between hydraulic fractures caused by the shrinkage of grains accompanying the increase of pore pressure and the other type of hydraulic fractures caused by intrusive fluids. He made the observation and proved by experiment that the shrinkage caused by pore pressure alone can form natural hydraulic fractures and preserve them open. By combining the Terzaghi effective stress and the constitutive equations of poroelasticity, he obtained the criterion of hydraulic shrinkage fracture formation in the basin. He concluded that vertical shrinkage fractures in a basin form preferably in less compressible rock and a lower thermal gradient, and the orientation of the fracture is controlled by the paleostress orientation. This is consistent with joints in the Appalachian Basin, which is the subject of this study.

Natural hydraulic fractures are commonly observed in source rocks, mainly black shale, in which a well-defined mechanical bed thickness is less common (Lash et al., 2004) (Figure 1). When clastic rocks overlying the source rock are charged by hydrocarbon migration, natural hydraulic fracturing develops. Examples are found in the Middle and Upper Devonian Catskill delta sediments of the Appalachian Basin (Engelder et al., 2009). Thus far, the spacing of natural hydraulic fractures is poorly understood compared with structural bending joints, and no method is available for

modeling their spacing distribution. In this paper, we develop a method that can be used to characterize the joint-saturation level in shale formations and potentially model natural hydraulic fractures in unconventional reservoirs on a reservoir scale.

Joint Spacing

In many geologic settings, joint spacing appears to correlate with mechanical bed thickness (Harris et al., 1960; McQuillan, 1973; Ladeira and Price, 1981; Huang and Angelier, 1989; Narr and Suppe, 1991; Gross, 1993; Gross et al., 1995; Ji and Saruwatari, 1998; Billi and Salvini, 2003). Spacing is also affected by the joint-propagation velocity, initial flaw distribution, and mechanical property contrast between beds (Fischer and Polansky, 2006). However, these observations apply mainly to structural bending joints in bedded sediments. In a different geologic scenario in which joints propagate under stress from the hydraulic shrinkage of the matrix grains (e.g., gas shale), spacing and its controlling parameters may be different.

This paper offers a solution to a long-standing geological problem: What is the best distribution to fit joint-spacing data regardless of the joint-driving mechanism? Further, how can the distribution fit parameter characterize the saturation of joints? Additionally, we try to answer several key questions concerning natural hydraulic fracturing: Is there a joint-spacing statistic that is characteristic of natural hydraulic fractures? Is the spacing of natural hydraulic fractures also proportional to mechanical bed thickness? If not, why? Last but not least, how can we use these findings to help develop unconventional reservoirs?

Joint-Saturation Level

Before getting into the details of joint-spacing analysis, an explanation of the concept of joint saturation is in order. Saturation is the state of joint density under which joint infilling ceases (Davis et al., 2011). Some use the ratio between bed thickness and joint spacing, which is called the fracture spacing index (FSI), or its inverse to estimate the level of joint saturation (Bai and Pollard, 2000). However, this parameter doesn't apply to the situation in which mechanical bed boundaries are not apparent, for example, a thick shale section or thick sandstone section (Rogers et al., 2004). Other attempts to estimate the joint-saturation level include using the fracture spacing ratio (FSR) (Becker and Gross, 1996) and standard deviation of joint spacing (Wu and Pollard, 1995, 2002). These methods are all limited to certain boundary conditions, and the joint-saturation level obtained using these methods cannot be compared from outcrop to outcrop, let alone from region to region.

Here, a more general interpretation of joint saturation is proposed. In elastic beds, the crack-driving tensile stress or strain decreases near an existing joint in a region called the "stress shadow" (Lachenbruch, 1961; Nur, 1982; Wu and Pollard, 1995; Becker and Gross, 1996). No new joints form within the stress shadow of a previous joint. In principle, the state of complete saturation of joints in a rock formation occurs when all the space is occupied by stress shadows associated with existing joints. The size of a stress shadow can differ dramatically according to different loading/boundary conditions and elastic properties. Therefore, the state of saturation does not necessarily have a correlation with joint density. In two extreme cases, a rock formation can have a low joint density but be saturated if stress shadows are wide (e.g., bedded sediments); similarly, it can have a high joint density but be undersaturated if stress shadows are narrow (e.g., gas shales) (Figure 2). The following discussion shows that these two extremes are common in nature. This paper develops a method that quantifies joint saturation in both cases.

METHOD

Distribution Fit of Joint Spacing

Many distribution fits characterize joint-spacing statistics with the ideal distribution fitting every situation. The most common distribution fits include log-normal distribution (Narr and Suppe, 1991), exponential distribution (Priest and Hudson, 1976;


(A)

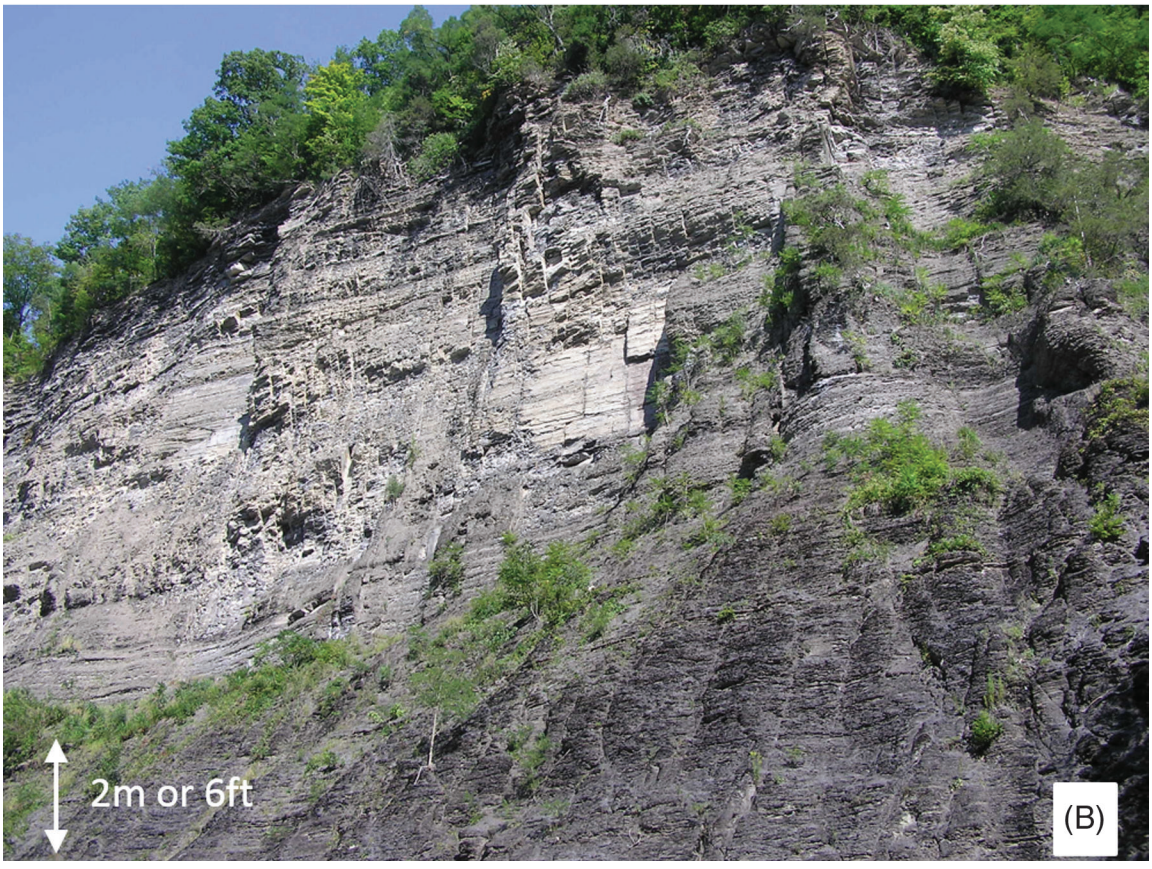
2m or 6ft
(B)

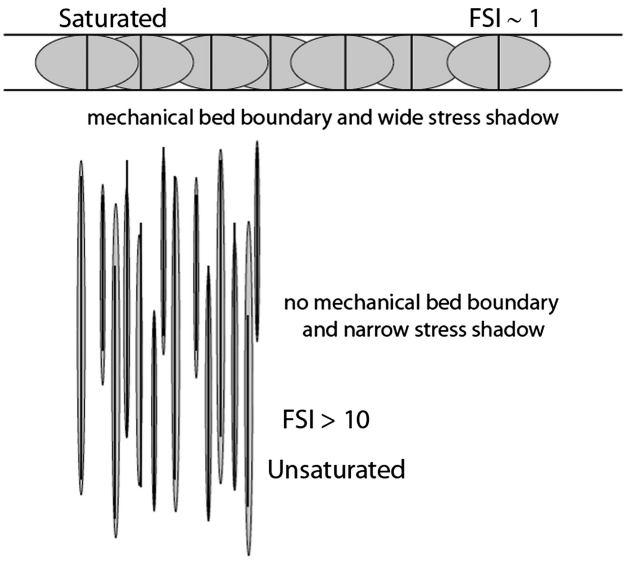

Figure 2. Low-density, saturated joints versus high-density, unsaturated joints. The upper panel represents structural bending joints in bedded sediments, whereas the lower panel represents natural hydraulic fractures in thick shale sections. Gray areas around joints are the stress shadows. Both are cross-section views. FSI = fracture spacing index.

Barton and Zoback, 1990), gamma distribution (Huang and Angelier, 1989; Gross, 1993), and Weibull distribution (Bardsley et al., 1990). Which one of these best fits joint-spacing statistics? In addition, how useful is this distribution for characterizing joint saturation? This study considers two cases: joint infilling in which the stress shadows are negligible and joint infilling between robust stress shadows. For a strict definition of "negligible" and "robust," see the Discussion section.

Where stress shadows are negligible, regardless of the joint-driving mechanism, joint infilling resembles a Poisson process. In probability theory, a Poisson process is a stochastic process that counts the number of events and the times at which these events occur in a given time interval (e.g., number of customers in a day). In the absence of stress shadows, joint infilling is distributed according to the three properties characteristic of a Poisson process: sparseness, independence, and stationarity (Ross, 2007). Sparseness means that few joints have grown relative to the space in which growth is possible. Independence means that the position of a subsequent joint does not depend on the position of previous joints. Stationarity means that joint infilling in one part of the rock resembles joint infilling along any other part of the same rock. Joint infilling governed by a Poisson process means the spacing has an exponential distribution. In probability theory, gamma and Weibull distributions are two-parameter (shape parameter α and scale parameter β) continuous probability distributions. Like exponential distributions, gamma and Weibull distributions are statistical analyses that further characterize the distribution of data. Both gamma and Weibull distributions are equivalent to an exponential distribution if their shape parameter α equals one, whereas a log-normal distribution can never approximate an exponential distribution. Hence, a log-normal distribution cannot accurately represent joint spacing in the presence of negligible stress shadows.

Where robust stress shadows exist, joint infilling is less probable within parts of the rock occupied by stress shadows. This voids the stationarity property, which makes infilling a nonhomogeneous Poisson process. In this case, the spacing distribution becomes complicated. We first examine the meaning of a stress shadow during infilling represented by a nonhomogeneous Poisson process.

A stress shadow is a region of relaxed stress next to a joint interface. The presence of a stress shadow will decrease the probability of infilling near existing joints. The probability density function (p) for infilling near an existing joint at a distance (x) is

$$p(x) = \lambda(x)e^{-\int_0^x \lambda(s)ds} \quad (1)$$

in which $\lambda(x)$ is an intensity function, and s is the integral variable. This function assumes that the

Figure 1. Picture of joints in gas shale. (A) Joints in the Union Springs Member of the Marcellus Shale near Cross Key, Pennsylvania. (B) Joints in the Geneseo Shale Member of the Genessee Formation at Taughannock Falls, New York State. These joints are natural hydraulic fractures generated by hydrocarbon maturation, resulting in an overpressured regime in the organic shales.

initial flaw distribution is uniform, and thus $\lambda(x)$ represents the driving stress as a function of the distance from a nearby pre-existing joint interface.

If $\lambda(x)$ is a hyperbolic function, the probability density function for infilling approximates a gamma distribution; likewise, if $\lambda(x)$ is a linear function, the probability density function for infilling approximates a Weibull distribution. Therefore, the final joint-spacing distribution will depend on the shape of the driving stress curve (Figure 3).

Direct data is not available on the in situ stress near an existing fracture. Therefore, the driving-stress curve of poroelastic shrinkage fracturing was modeled using the finite-element method (Fischer et al., 1995), which is assumed a good approximation of nature. In Figure 3, we overlay the hyperbolic function, linear function, and the simulated result of crack-driving stress from Fischer et al. (1995). The hyperbolic function is a better approximation for the driving-stress curve, because, in nature, the slope of driving stress is continuous. For this reason, the gamma-distribution fit is preferred to the Weibull distribution fit for characterizing joint saturation.

Joint saturation is a condition in which joint infilling is no longer possible. It has been widely observed

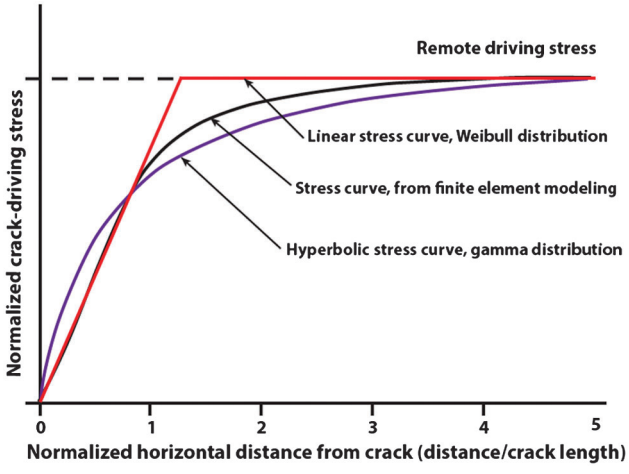

Figure 3. Plot of normalized crack-driving stress versus normalized horizontal distance from the crack. The three curves labeled are the stress simulated from finite-element modeling (Fischer et. al. 1995), the linear stress curve for Weibull distribution, and the hyperbolic stress curve for gamma distribution. We can see that the gamma distribution is a better approximation of the finite-element modeled case, which we take as the best approximation of nature.

that, as joints near saturation in rock, the shape of the joint-spacing histogram tends to migrate from skewed to symmetric (Rives et al., 1992). As joints infill to saturate the rock, skewness of the joint-spacing histogram decreases from the extreme represented by an exponential distribution. To express joint-spacing data, a distribution fit should have the ability to characterize the change of skewness, something an exponential distribution can not do as the skewness of an exponential distribution is always two.

The gamma-distribution probability density function (g) (not to be confused with g, acceleration due to gravity) is written in terms of the shape parameter (α) and scale parameter (β) according to

$$g(x;\alpha,\beta)=\frac{\beta^{\alpha}x^{\alpha-1}e^{-\frac{x}{\beta}}}{\Gamma(\alpha)}(x>0) \qquad (2)$$

in which x is the independent variable, and $\Gamma(\alpha)$ is the gamma function

$$\Gamma(\alpha)=\int_0^{\infty}x^{\alpha-1}e^{-x}dx$$

The skewness of a gamma distribution can be written as

$$\text{Skewness}=\frac{2}{\sqrt{\alpha}} \qquad (3)$$

The shape parameter of gamma distribution alone is sufficient to characterize the skewness and, hence, the saturation of joints. This is another reason the gamma distribution is preferred over the Weibull distribution, as the skewness of a Weibull distribution requires both shape and scale parameters. The following sections include a test of the suitability of using the gamma-distribution shape parameter (α) in representing the joint-saturation level by numerical simulation. The saturation level is then used to distinguish between natural hydraulic fractures and structural bending joints in gas shale and bedded sediments, respectively.

Numerical Simulation of Joint Spacing in a Range between Negligible and Robust Stress Shadows

Previous studies have shown that joint spacing is strongly controlled by stress shadows (Narr

and Suppe, 1991; Rabinovitch and Bahat, 1999). Therefore, understanding the effect of stress shadows on the joint-spacing distribution is critical to interpreting joint-driving mechanisms. Numerical simulations of the joint-infilling process were used to understand the specific effect of stress-shadow width on the development of joint-spacing distributions.

Several theoretical models calculate the stress/strain field in the rock around an existing joint. These include the stress-transfer model (Hobbs, 1967; Narr and Suppe, 1991), the stress-reduction model (Pollard and Segall, 1987), and the stress-transition model (Bai et al., 2000). These models are all mathematically complex and restricted to certain boundary conditions. To avoid this inherent complexity, a non-varying stress shadow is maintained during each run of 50 infilling events.

A conventional, sequential-filling, one-dimensional (1-D) numerical simulation generates joint-spacing data (Rives et al., 1992) (Figure 4). Each run of the simulation starts with an empty scan line with a length of 100 m (328 ft). We randomly generate 50 joints with the same fixed stress shadow and drop them on the scan line. The locations of joints are random and follow a uniform distribution. Uniform distribution is a reasonable hypothesis under the assumption that no pre-existing fault zones or other local stress mechanisms are present on the scan line. The width of the stress shadow (i.e., the width of the zone adjacent to an existing joint in which new joints are excluded) is increased from 0 to 1 m (3.28 ft) in increments of 0.01 m (0.4 in.). Any later joint that is placed within the stress shadow of any previously formed joint will be excluded. This process is repeated until all 50 joints have grown outside existing stress shadows. Here, the average joint spacing is the length of the scan line divided by the number of joints, or 2 m (6.6 ft). Afterward, the record of the spacing between each of the 50 joints is plotted as a histogram. A gamma distribution is fit to each histogram, and the

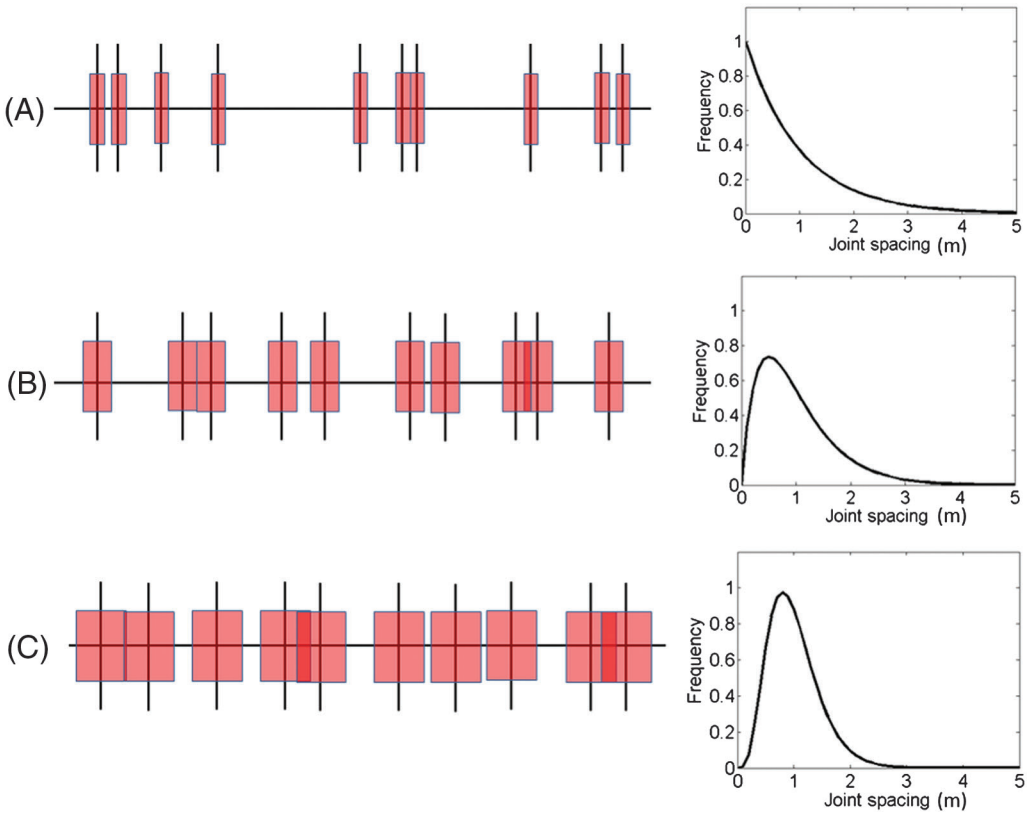

Figure 4. Illustration of the 1-D sequential-filling modeling of the joints. The vertical black lines are joints. The red boxes are stress shadows, the widths of which are proportional to the size of stress shadow. The distribution fit to the spacing histogram is shown in the boxes to the right. (A), (B), and (C) show three scenarios in which the size of stress shadow increases, with (A) representing the smallest (negligible) stress shadows and (C) representing the largest (robust) stress shadows. The distribution fit evolves from asymmetric to symmetric. These distribution fits are only shown for illustration purposes. The joint-spacing data are not from the scan line on the left.

shape parameter is recorded for each run of the simulation.

A new parameter called the joint-saturation ratio (JSR) is defined:

$$\text{JSR} = (\text{size of stress shadow}/\text{average spacing of joints}) \times 100(\%) \quad (4)$$

Importantly, the JSR is independent of joint height and mechanical bed thickness. Therefore, the JSR can be used for both structural bending joints, where mechanical bed thicknesses commonly occur, and natural hydraulic fractures in gas shales, which grow independently of any apparent mechanical bed thickness. If no stress shadow is present, the JSR is zero. If the size of the stress shadow is 0.5 m (1.64 ft) and the average spacing of joints is 2 m (6.6 ft) (in our simulated case), the JSR is 0.5/2.0*100% = 25%. In our simulation, the JSR increased from 0% to 50%.

Shape parameter versus JSR is plotted for the entire simulation (Figure 5). The shape parameter of the gamma-distribution fit is scattered at each JSR value. One major reason for this is the overlapping between the stress shadows of adjacent joints. The influence of overlapping stress shadows is negligible when the JSR is small, but it can be significant when JSR is large. For example, if the JSR is

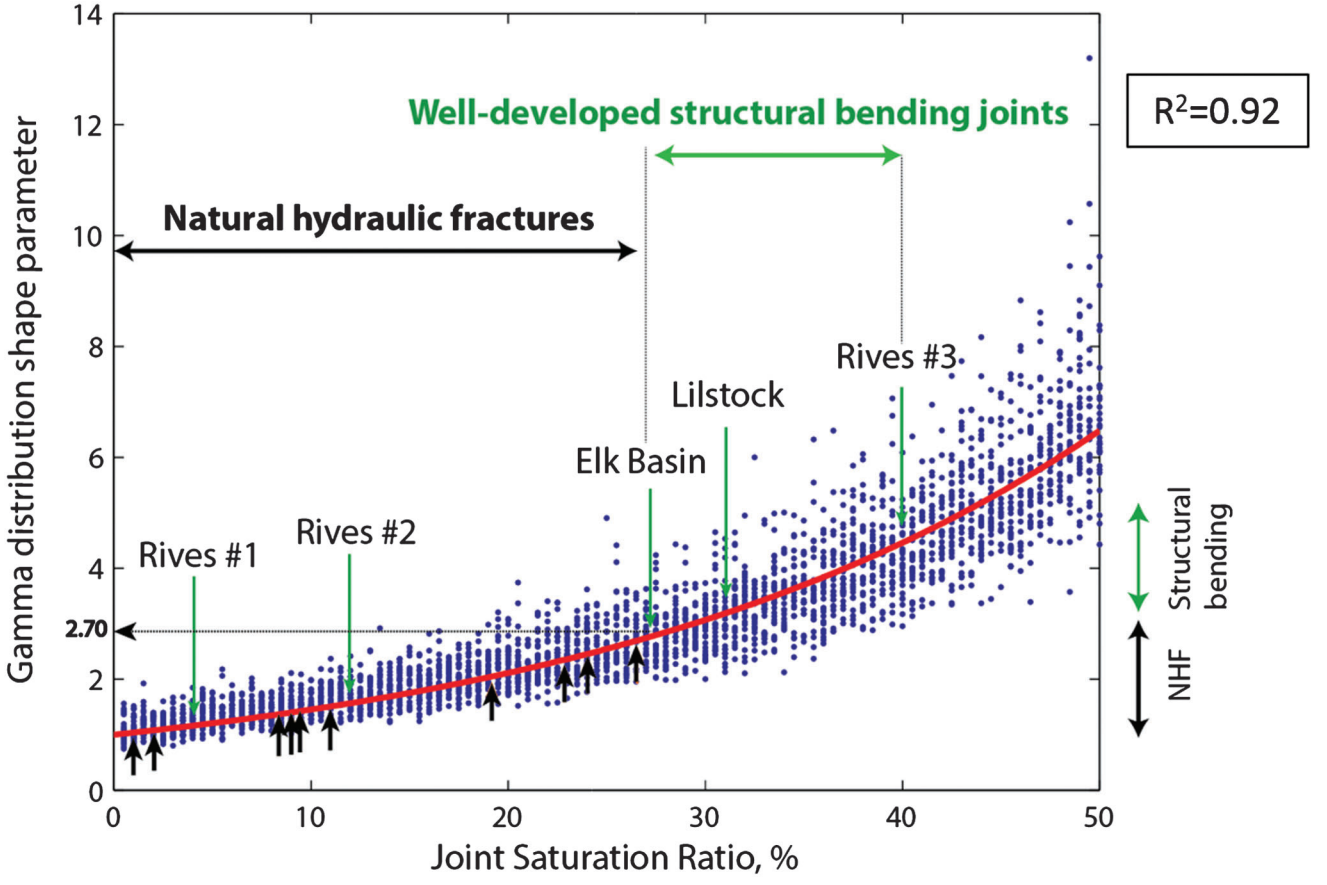

Figure 5. Plot of the numerical simulation results: shape parameter of the gamma-distribution fit of joint spacing versus the joint-saturation ratio (JSR). The curve in red is the function $y = 42^x$ which is the best-fit curve to the data points. Natural hydraulic fracture data collected in the Appalachian Basin are represented by black arrows pointing to the curve, whereas those of well-developed structural bending joints are represented by green arrows pointing to the curve. Rives experiments 1 and 2 are represented by red arrows because they fall in neither of the two categories above. The range of JSR in both natural hydraulic fractures and well-developed structural bending joints (Elk Basin, Lilstock, and Rives Experiment 3) are highlighted. The area for natural hydraulic fracture (NHF) and structural bending are empirical and open to change. The points become dispersed as the JSR increases because we did not consider the overlapping of neighbor stress shadows when calculating JSR.

50% (i.e., the stress shadow is 1 m [3.3 ft] in our simulation) at one extreme in which the stress shadows never overlap, the entire scan line is occupied. At the other extreme, in which all the stress shadows overlap, half of the scan line is still available for further joint growth. This is why the simulation was stopped at a JSR of 50%. In this sense, JSR as a parameter to characterize the saturation level of joints in the rock is limited. However, JSR is simple to use and easy to understand. In the real world, a stress shadow is not a definite region where absolutely no joint can grow; rather it is a region with reduced probability of joint initiation as shown in the previous section (Distribution Fit of Joint Spacing). In our simulation, to overcome the scattering effect, we did 30 realizations to reduce the uncertainty caused by overlapping. The regression curve, shown in Figure 5, averages the scattering effect.

The gamma-distribution shape parameter and the JSR (Figure 5) are positively correlated. The skewness of the gamma distribution can be represented by a shape parameter alone. This is consistent with the previous conclusion that, as joints saturate the rock, the skewness of the histogram decreases. Therefore, if the shape parameter of joint spacing from data is known, the JSR can be identified from the regression function shown in Figure 5. This JSR is of use in characterizing the joint saturation of both natural hydraulic fractures and structural bending joints.

RESULTS AND DATA ANALYSIS

Spacing of Structural Bending Joints in Bedded Sediments

To test our hypothesis that the shape parameter (hence, JSR) represents the degree of joint saturation, three structural bending joint data sets published in the literature are analyzed: Lilstock (Engelder and Peacock, 2001), Elk Basin (Engelder et al., 1997), and a thin-plate bending experiment (Rives et al., 1992). A number of studies have shown that the spacing of well-developed structural bending joints should be about the same as mechanical bed thickness (i.e., FSI = 1) (Narr and Suppe, 1991; Gross, 1993; Ji et al., 1998; Fischer and Polansky, 2006). Bai and Pollard (2000) further proposed four ranges of joint saturation based on FSI value (FSI < 0.83 undersaturated; 0.83 < FSI < 1.25 saturated; 1.25 < FSI < 3.3 supersaturated; FSI > 3.3, hypersaturated) (Bai and Pollard, 2000; Davis et al., 2011).

For Lilstock and Elk Basin joints, the original spacing data were used. Three outcrops from each structure where scan-line data sets exceeded 30 joints were selected to compare with our natural hydraulic fracture data from the Appalachian Plateau. The joint spacing of the bending plate experiment Rives conducted was taken from a published figure. The FSI for Elk Basin and Lilstock is well documented (Engelder et al., 1997; Engelder and Peacock, 2001). The plate in the Rives experiment was 1.5 mm (0.06 in.) thick. We divided the plate thickness by the median joint spacing to get the FSI. The shape parameters, JSR and FSI for structural bending joints, are listed in Table 1.

The thin-plate bending experiment best illustrates the evolution of joint saturation by the gamma-distribution shape parameter (Rives et al., 1992). In the experiment, the authors simulate structural bending by putting a thin plate of polystyrene into a four-point bending apparatus. At different stages of bending, the joints were counted. In stage 1, 65 joints occurred within the plate. The shape parameter of the gamma-distribution fit to the joint spacing is 1.17, corresponding to a JSR of 4.09%. In stage 2, 109 joints occurred. The shape parameter increased to 1.58, corresponding to a JSR of 12.26%. Eventually, the joint number reached 140 with a shape parameter of 4.48, and the JSR increased to 40.09%. The authors called these three stages low density, intermediate density, and high density. Meanwhile, the FSI increased from 0.15 to 0.74 to 1.18. The evolution of both the shape parameter and the FSI is consistent. This proves that the shape parameter is at least as good an indicator of joint saturation as FSI.

Both Lilstock and Elk Basin data were collected from joint sets on an anticline. Elk Basin is located on the Wyoming–Montana border. It is a basement-cored anticlinal structure of Laramide age inside the Big Horn Basin of Wyoming. The section exposed for joint analysis consists of several formations of the Campanian (Upper Cretaceous) section deposited on the foreland of the Sevier orogenic belt. Lilstock is located on the south side of the Bristol Channel,

Table 1. Spacing Statistics of Structural Bending Joints in Bedded Sandstone/Siltstone (Elk Basin, Lilstock, and Rives Plate Bending Experiment)*

Name of Outcrop/Experiment	Shape Parameter	JSR, %	Bed Thickness (cm)	FSI
Elk Basin Judith River Station 18	2.75	27.02	35.49	1.34
Elk Basin Judith River Station 20	2.75	27.05	64.94	1.15
Elk Basin Eagle A Station 11	3.19	31.01	41.42	0.66
Lilstock Outcrop 1921	3.40	32.80	19.00	0.34
Lilstock Outcrop 1848 m3	3.04	29.74	18.00	0.95
Lilstock Outcrop 497	3.15	30.67	27.00	0.44
Rives Experiment Stage 1	1.17	4.09	0.15	0.15
Rives Experiment Stage 2	1.58	12.26	0.15	0.74
Rives Experiment Stage 3	4.48	40.09	0.15	1.18
Average of well- developed joints	3.25	31.20	–	0.87

*JSR = joint-spacing ratio; FSI = fracture spacing index (median bed thickness/median spacing).

England. Lilstock is an inversion structure in the Alpine foreland. The section exposed for joint analysis consists of the Sinemurian (Early Jurassic) Blue Lias limestone deposited on the Tethyian margin of Europe.

The situation is similar to the thin-plate structural bending experiment. Observed from these data, the well-developed structural bending joints generally have a large shape parameter (>2.7), hence, a high JSR (>26.5%). The JSR is fairly constant around 30% for well-developed structural bending joints (Table 1).

The Elk Basin and the Lilstock data sets are inconsistent relative to the Rives bending-plate data set (Table 1). The data with the highest FSI for both Elk Basin and Lilstock have the lowest JSR, which is inconsistent with preconceived notions. This observation may be explained a couple of ways: First, transforming the shape parameter to a JSR is uncertain (as shown in Figure 5) because of overlapping stress shadows from adjacent joints. Second, the statement that FSI reflects joint-saturation level is based on the assumption that the width of the stress shadow is proportional to bed thickness, and the ratio holds constant, which is not necessarily true in nature. The width of stress shadows is affected by the contrast of mechanical properties between beds. The mechanical properties of the beds are very likely to be heterogeneous spatially. If the rock properties are not uniform, FSI may not accurately reflect the degree of joint saturation. The homogeneity of the plate in the Rives experiment is the reason FSI works, as the above factors do not affect it. In this sense, the shape parameter (hence, JSR) is a better indicator than FSI for joint saturation, as the assumption of a relationship between stress-shadow width to bed thickness is not required.

Furthermore, the JSR of Elk Basin and Lilstock are both around 30% despite their evolution in different tectonic settings. Based on our observations so far, this JSR may represent a limit to infilling of structural bending joints in nature. The FSI is more scattered in adjacent outcrops, which means it is a less stable measure of joint saturation in each tectonic setting. In conclusion, the shape parameter and, hence, the JSR, is better able to characterize joint saturation for structural bending joints in bedded sediments.

Spacing of Natural Hydraulic Fractures in the Middle and Upper Devonian Section of the Appalachian Basin

To test the JSR method on the distribution of natural hydraulic fractures, joint-spacing data were gathered from outcrops in the Middle and Upper Devonian section of the Catskill delta in northeast Pennsylvania and central New York State (Figure 6). These sediments were deposited during the Acadian orogeny (Ettensohn, 1987). Most of these data come from road cuts, waterfalls, and gullies around lakes (Figure 7). All of these outcrops have more than 30 joints and minimal erosion to allow a sufficient sampling of joint spacing. Some of these outcrops only

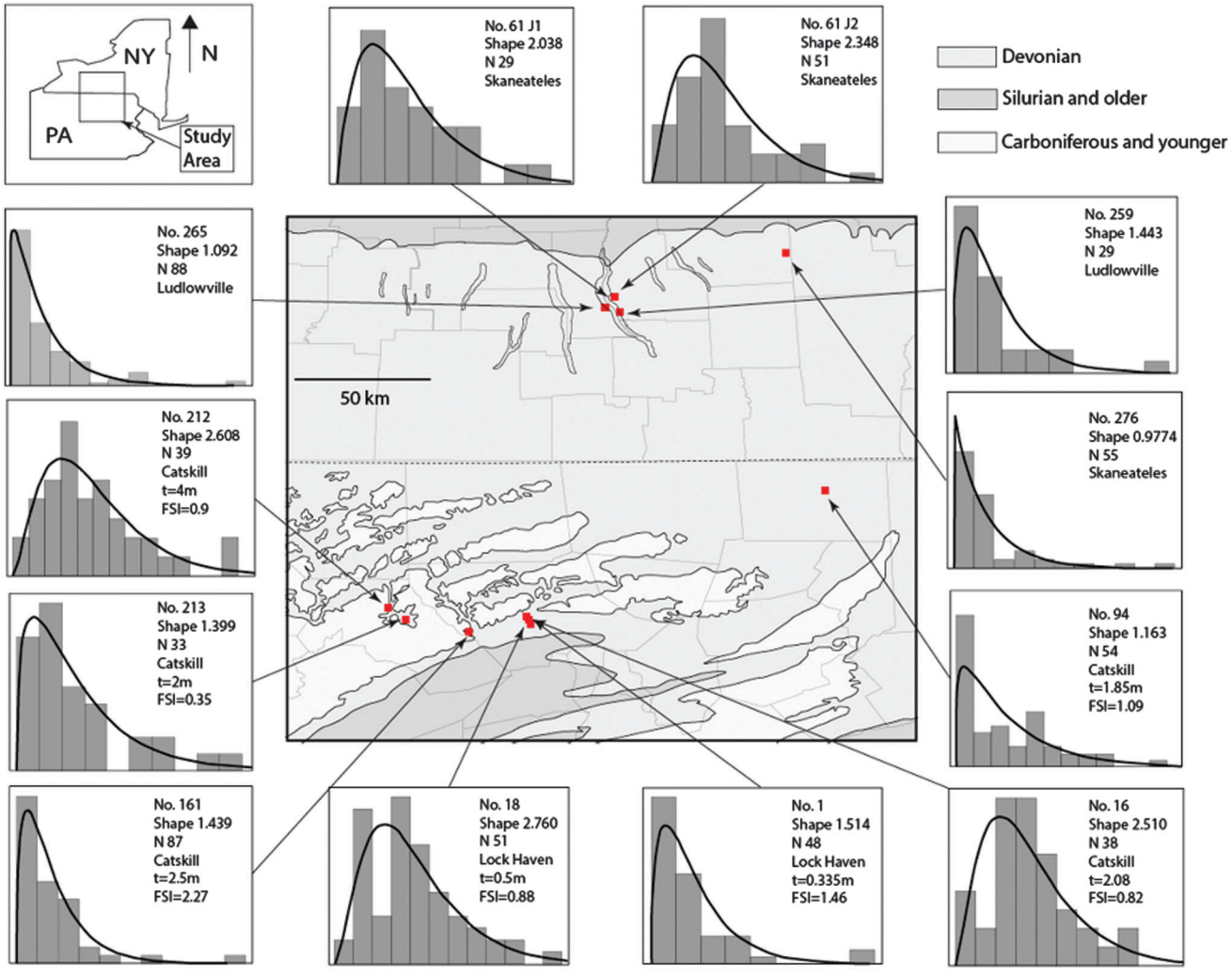

Figure 6. Histograms of the selected outcrops in the Appalachian Basin showing joint spacing with gamma-distribution fits. The squares are the locations of outcrops listed in Table 2. Ludlowville, Skaneateles, Catskill, and Lock Haven are formation names in the Devonian section of the Appalachian Basin.

have a pavement surface available. Hence, bed thickness cannot be measured. Some of the blanks in the "bed thickness column" in Table 3 are a manifestation of this, whereas other blanks are the result of joints of immeasurable height. Data also come from the Middlesex Shale Member of the Sonyea Formation near Keuka Lake and the Geneseo Shale Member of the Genesee Formation near Seneca Lake, New York (Hagin, 1997).

Northeast Pennsylvania has been an actively explored area for shale gas. The Marcellus Formation in this region is among the largest shale-gas plays in the world (Engelder and Lash, 2008). Evidence indicates that the joints present are driven by poroelastic shrinkage during natural hydraulic fracturing at the time of natural-gas generation and migration (Lacazette and Engelder, 1992; Carter et al., 2001; Lash et al., 2004).

Natural hydraulic fractures are hosted by both bedded sandstone–siltstone–shale sequences (Table 2) and more homogeneous black shales (Table 3). These two fundamentally different stratigraphic packages show different patterns regarding FSI and JSR. The FSI (Figure 8A) and JSR (Figure 8B) of structural bending joints are compared with those for natural hydraulic fractures in both stratigraphic packages.

The black shale is generally thick (>5 m [>16 ft]) and lacks apparent mechanical boundaries at the scale

Figure 7. Example of joint-spacing measurement in the field. (A) is at Moonshine Falls, New York State, with Yunhui Tan for scale (No. 61 in Figure 6). (B) is along Road 120 in Clinton County, Pennsylvania with Thomas Johnston for scale (No. 212 in Figure 6).

Table 2. Spacing Statistics of the Bedded Natural Hydraulic Fractures in the Appalachian Basin*

Outcrop No.	Shape Parameter	JSR, %	Bed Thickness (m)	FSI	Latitude	Longitude
1	1.51	11.10	0.34	1.46	41.29292 N	77.06672 W
16	2.51	24.62	2.08	0.82	41.30618 N	77.0758 W
18	2.76	27.16	0.50	0.88	41.27166 N	77.0572 W
94	1.16	4.04	1.85	1.09	41.86640 N	75.7533 W
161	1.44	9.74	2.50	2.27	41.24035 N	77.3307 W
212	2.61	25.65	4.00	0.90	41.34679 N	77.6885 W
213	1.40	8.98	2.00	0.35	41.29494 N	77.6112 W
Average	1.91	15.90	–	1.11		

*Locations are shown in Figure 6. JSR = joint-spacing ratio; FSI = fracture spacing index (median bed thickness/median spacing).

of the outcrop. The spacing of joints is mostly on the order of tens of centimeters, and calculation of FSI results in extremely high numbers (>50). In this case, the FSI implies the joints are hypersaturated (Bai and Pollard, 2000) with results far higher than are reasonable for structural bending joints. However, we can see from Table 3 and Figure 8B that the JSR inferred from the shape parameters of the shale outcrops range from near 0 to 30%. The average JSR is 14.55%, which implies a lower joint saturation than the well-developed structural bending joints and is within the statistical norm.

The natural hydraulic fractures in bedded rocks have an average JSR of 15.9% and an average FSI of 1.11 (Table 2). The natural hydraulic fractures in bedded rocks have a range of FSI that is slightly higher than structural bending joints (Figure 8A). However, the JSRs for these same natural hydraulic fractures are much lower than those of structural bending joints (Figure 8B). This difference separates infilling distribution for natural hydraulic fracturing from infilling for structural bending. This implies that natural hydraulic fractures have a small (sometimes even negligible) stress shadow relative to joint height (i.e., mechanical bed thickness) when compared with structural bending joints with robust stress shadows.

The ranges of JSR of natural hydraulic fractures in bedded and homogeneous rocks are about the same (Figure 8B). This, again, suggests that shape parameter (hence, JSR) is a more powerful, more universal parameter to represent the joint saturation in rocks regardless of lithology and driving mechanism.

Table 3. Spacing Statistics of Unbedded Natural Hydraulic Fractures in the Appalachian Basin. Locations are Shown in Figure 6*

Outcrop No.	Shape Parameter	JSR, %	Bed Thickness (m)	FSI	Latitude	Longitude
61J2	2.40	23.41	–	–	42.72723 N	76.6860 W
61J1	2.04	19.05	–	–	42.72723 N	76.6860 W
276	0.98	–	–	–	41.62087 N	75.7788 W
259	1.44	9.81	–	–	41.46800 N	75.6686 W
265	1.10	2.35	–	–	41.37664 N	75.6685 W
263	0.78	–	–	–	41.38573 N	75.6615 W
266	1.07	1.86	–	–	41.37294 N	75.6774 W
SEN-11-PG-2/J1	1.52	11.00	–	–	–	–
SEN-11-PG-3/J1	2.72	26.76	–	–	–	–
STE-01-AY-2/J1	2.68	26.39	–	–	–	–
STE-01-AY-3/J1	1.47	10.29	–	–	–	–
Average	1.82	14.55	–	–	–	–

*The last four outcrops are from Hagin (1997), which are not indicated on Figure 6. JSR = joint-spacing ratio; FSI = fracture spacing index (median bed thickness/median spacing).

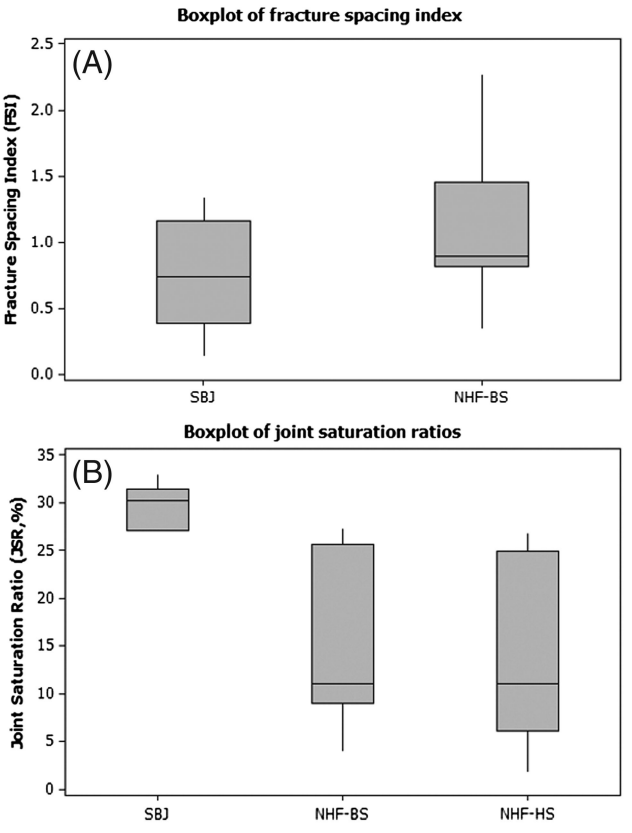

Figure 8. (A) Boxplot of the fracture spacing index (FSI) for structural bending joints in bedded sediments and natural hydraulic fractures in bedded sediments. (B) Boxplot of joint-saturation ratio (JSR) for structural bending joints in bedded sediments, natural hydraulic fractures in bedded sediments, and natural hydraulic fractures in homogeneous shale section. The gray bars are the interquartile range. The vertical lines are the outlier range. The horizontal lines are the median values. The data are in Tables 1, 2, and 3. SBJ = structural bending joints; NHF-BS = natural hydraulic fractures in bedded sediments; NHF-HS = natural hydraulic fractures in homogeneous shale. The natural hydraulic fractures in homogeneous shale were not plotted in (A) because their FSI is too large (>50).

Although the stress shadow from natural hydraulic fracturing is smaller compared with structural bending joints (Figure 2), the joint density in black shale can reach the level at which stress shadows affect the spacing. The fact that two data points (SEN-11-PG-3/J1 and STE-01-AY-2/J1) from the Middlesex and Geneseo units, measured by Hagin (1997), reached a JSR of nearly 30% (Table 3) is a manifestation of this phenomenon.

Two outcrops (numbers 276 and 263) have shape parameters less than one (Table 3). Theoretically, this is not possible. If joint infilling is a Poisson process, the spacing should follow an exponential distribution, which means the shape parameter equals one. However, the assumption of uniform flaw distribution may not occur in all outcrops if a zone of high natural flaw concentration occurs, for example. Only two outcrops have a shape parameter less than one. This suggests that a uniform flaw distribution is a reasonable assumption for joint infilling leading to a gamma distribution for joint spacing.

DISCUSSION

Negligible and Robust Stress Shadows

To define the extent to which stress shadows are negligible, we ran a chi-square test for the exponential distribution on the gamma-distribution data. By using a 5% significance level, when the gamma-distribution shape parameter is between 1 and 1.18, it is equivalent to an exponential distribution. A gamma-distribution shape parameter between 1 and 1.18 is the same as a JSR between 0 and 4.43%. Therefore, any stress shadow that is smaller than 4.43% of the mean joint spacing will be considered negligible. Any stress shadow larger than 4.43% of the mean joint spacing is, therefore, robust.

Interference between Natural Hydraulic Fracturing and Structural Bending

We treat the joints in the Elk Basin and Lilstock localities as having formed from purely structural bending, one end member of the joint-driving mechanism. Conversely, we treat the joints in the Appalachian Basin as having formed solely from natural hydraulic fracturing, the other end-member joint-driving mechanism. However, it is possible that both mechanisms were factors. Yet, treating them as end members is reasonable in our case for the following reasons: (1) Structural bending joints have a larger stress shadow than natural hydraulic fractures. In the case of Elk Basin or Lilstock, even if the formation was overpressured when the joints were formed, the stress shadow from a structural bending joint-driving mechanism will still dominate. (2) The joints observed in the Appalachian Basin are majority

cross-fold joints (i.e., perpendicular to the folding axis). Therefore, structural bending is not the dominating mechanism. Although oroclinal bending was present when the joints were formed, it likely acted more as a remote, regional stress field rather than a local, driving stress around a fracture (Engelder and Geiser, 1980).

General Application of JSR

The method proposed in this paper provides a way to estimate joint-saturation level independent of bedding thickness effects. This unique property extends the assessment of joint saturation from outcrop to the subsurface reservoir. Image logs provide the most reliable means to visualize fractures in the reservoir, in particular, horizontal borehole image logs provide a good sampling of systematic vertical fracture sets (Waters et al., 2006). However, in the horizontal image log, mechanical bedding thickness can rarely be determined because of borehole size limitations, which renders the FSI method impractical. Our JSR method is advantageous in this regard.

Relevance to Hydraulic Fracturing of Unconventional Reservoirs

Our JSR method can be applied to the development of unconventional resources in two major aspects. First, JSR can help distinguish drilling-induced fractures from natural fractures. We used the horizontal image log data from (Waters et al., 2006) and ran a JSR calculation on the induced fractures (Figure 9). The JSR obtained on the drilling-induced fractures from this figure is about 44%, which is higher than found in natural hydraulic fractures. Therefore, fracture sets in the wellbore with abnormally high JSR are unlikely to be natural hydraulic fractures. We think the reason drilling-induced fractures have such a high JSR is that drilling imparts large rock stresses. Every area immediately outside a stress shadow of a previous fracture will be induced, creating an artificially high joint-saturation level.

Second, JSR can be used to help understand the heterogeneity of fracture distribution in the shale reservoir. We have shown that the stress shadows of natural hydraulic fractures are relatively small, especially in the shale sections; therefore, joint spacing in shales will always be very heterogeneous. To illustrate this, we ran a random generation of joints using a gamma distribution with a shape parameter of 1.5 (JSR 11%), which is a typical value of natural hydraulic fractures in shales (Table 3). Again, we used a 100-m (328-ft) scan line, but this time threw 100 joints on it for accuracy purposes (Figure 10). Ideally, the mean joint spacing should be 1 m (3.28 ft). An average number of joints per 5 m (16 ft) was calculated using a moving-average

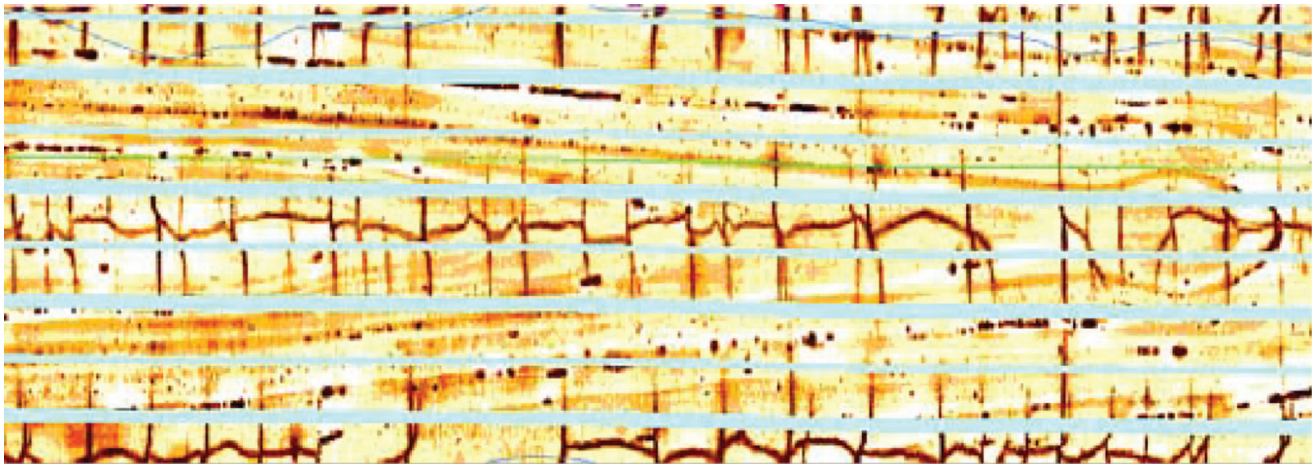

Figure 9. Example of an FMI image log in a horizontal wellbore from the Mississippian Barnett Shale in Fort Worth Basin. Picture is obtained from Waters et. al. (2006, Figure 4) with permission from the Society of Petroleum Engineers. Drilling-induced fractures are vertical in the image. Natural fractures are obliquely intersected by the wellbore. The joint-saturation ratio (JSR) of the drilling-induced fractures is approximately 44%, which is far higher than a JSR from a typical natural fracture.

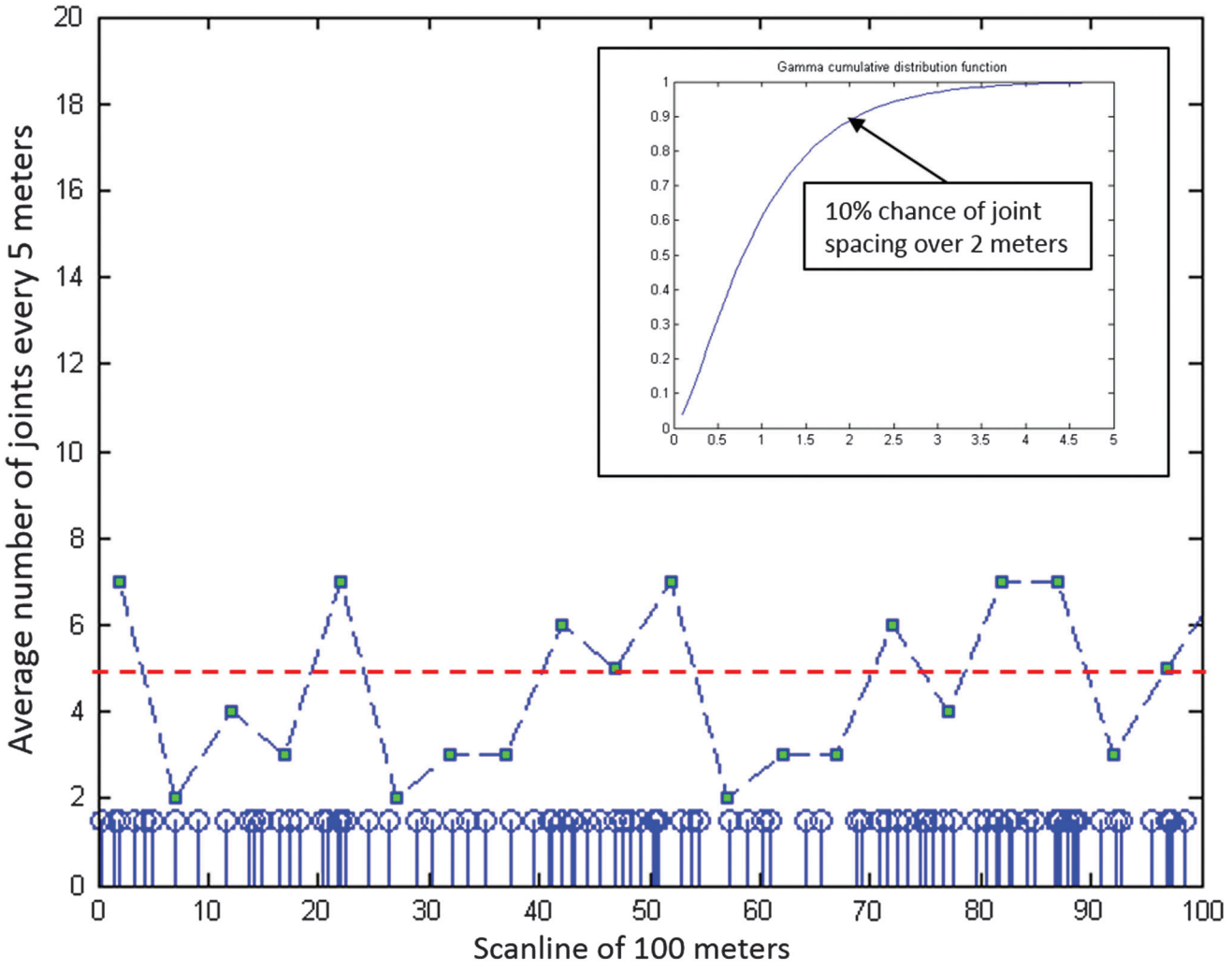

Figure 10. Example of using the joint-saturation ratio concept to simulate natural fracture distribution in gas shale. The short blue lines with circles at the top indicate the simulated joints. One hundred joints exist on the 100-m (328-ft) scan line. The dashed blue line is showing the average number of joints every 5 m (16 ft). Average number of joints should be five (red dashed line), but the number of joints actually varies dramatically along the scan line. The inset graph is showing the cumulative probability curve of joint spacing with a gamma-distribution shape parameter of 1.5.

window on the scan line and plotted (Figure 10). Although the expected number of joints per 5 m (16 ft) is five, we can see from Figure 10 that it can get as low as two and as high as seven. If development geologists understand both the JSR and mean joint spacing in the reservoir, they can simulate different scenarios and help determine perforation and stage spacing accordingly. Modern hydraulic fracturing simulation software like Mangrove® requires natural fracture models to simulate the propagation of hydraulic fractures. The JSR provides a critical geological constraint on the creation of natural fracture models.

CONCLUSIONS

1. Gamma distribution is the most appropriate distribution fit for joint spacing considering the width of stress shadows. The joint saturation ratio (i.e., shape parameter of the gamma-distribution fit) is a universal indicator of the degree of joint saturation regardless of lithology or driving mechanism.
2. Compared with well-developed structural bending joints, the natural hydraulic fractures in the Middle and Upper Devonian sections of the Appalachian Basin have a smaller joint-saturation ratio (JSR), hence, a lower degree of joint saturation. Another difference is that the spacing of natural hydraulic

fractures in gas-shale sections is not proportional to the bed thickness. This is related to the variable size of stress shadows associated with different driving mechanisms and boundary conditions.

3. In the case of joints driven by joint-normal stretching during structural bending, the stress shadows are wide and infilling reaches a JSR of 30%, which approximates complete saturation. In the case of joints driven by poroelastic shrinkage during natural hydraulic fracturing, the stress shadows are much narrower, and infilling commonly falls short of a JSR of 30%, which means the joint sets have not reached complete saturation.

REFERENCES CITED

Bai, T., and D. D. Pollard, 2000, Fracture spacing in layered rocks: A new explanation based on the stress transition: Journal of Structural Geology, v. 22, no. 1, p. 43–57.

Bai, T., D. D. Pollard, and H. Gao, 2000, Explanation for fracture spacing in layered materials: Nature, v. 403, no. 6771, p. 753–756.

Bardsley, W., T. Major, and M. Selby, 1990, Note on a Weibull property for joint spacing analysis: International Journal of Rock Mechanics and Mining Sciences, v. 27, p. 133–134.

Barton, C., and M. Zoback, 1990, Self-similar distribution of macroscopic fractures at depth in crystalline rock in the Cajon Pass scientific drillhole, *in* N. Barton and O. Stephansson, eds., Rock joints: Proceedings of a regional conference of the International Society for Rock Mechanics, Loen, Norway, June 4–6, 1990, Rotterdam, A. A. Balkema, p. 163–170.

Becker, A., and M. R. Gross, 1996, Mechanism for joint saturation in mechanically layered rocks: An example from southern Israel: Tectonophysics, v. 257, p. 223–237.

Billi, A., and F. Salvini, 2003, Development of systematic joints in response to flexure-related fibre stress in flexed foreland plates: The Apulian forebulge case history, Italy: Journal of Geodynamics, v. 36, no. 4, p. 523–536.

Carter, B. J., A. R. Ingraffea, and T. Engelder, 2001, Natural hydraulic fracturing in bedded sediments, International Association for Computer Methods and Advances in Geomechanics: Annual Meeting, Tucson, Arizona, p. 1–10.

Chopra, S., and K. Marfurt, 2007, Curvature attribute applications to 3D surface seismic data: The Leading Edge, v. 26, no. 4, p. 404–414.

Davis, G. H., S. J. Reynolds, and C. F. Kluth, 2011, Structural Geology of Rocks and Regions, 3rd ed.: Canada, John Wiley & Sons, Limited, p. 223–225.

Engelder, T., and P. Geiser, 1980, On the use of regional joint sets as trajectories of paleostress fields during the development of the Appalachian Plateau, New York: Journal of Geophysical Research, v. 85, no. B11, p. 6319–6341.

Engelder, T., and A. Lacazette, 1990, Natural hydraulic fracturing, *in* N. Barton and O. Stephansson, eds., Rock joints: Proceedings of a regional conference of the International Society for Rock Mechanics, Loen, Norway, June 4–6, 1990, Brookfield, A. A. Balkema, p. 35–43.

Engelder, T., and M. P. Fischer, 1996, Loading configurations and driving mechanisms for joints based on the Griffith energy-balance concept: Tectonophysics, v. 256, no. 1–4, p. 253–277.

Engelder, T., M. R. Gross, and P. Pinkerton, 1997, An analysis of joint development in thick sandstone beds of the Elk Basin anticline, Montana-Wyoming: Fractured reservoirs: Characterization and modeling: Denver, Colorado, Rocky Mountain Association of Geologists, p. 1–18.

Engelder, T., and D. C. P. Peacock, 2001, Joint development normal to regional compression during flexural-flow folding: The Lilstock buttress anticline, Somerset, England: Journal of Structural Geology, v. 23, no. 3, p. 259–277.

Engelder, T., and G. G. Lash, 2008, Marcellus Shale play's vast resource potential creating stir in Appalachia: The American Oil & Gas Report, v. 52, no. 6, p. 76–87.

Engelder, T., G. Lash, and R. S. Uzcátegui, 2009, Joint sets that enhance production from Middle and Upper Devonian gas shales of the Appalachian Basin: AAPG Bulletin, v. 93, no. 7, p. 857–889.

Ettensohn, F. R., 1987, Rates of relative plate motion during the Acadian orogeny based on the spatial distribution of black shales: The Journal of Geology, v. 95, no. 4, p. 572–582.

Fischer, M. P., M. R. Gross, T. Engelder, and R. J. Greenfield, 1995, Finite-element analysis of the stress distribution around a pressurized crack in a layered elastic medium: Implications for the spacing of fluid-driven joints in bedded sedimentary rock: Tectonophysics, v. 247, no. 1–4, p. 49–64.

Fischer, M. P., and A. Polansky, 2006, Influence of flaws on joint spacing and saturation: Results of one-dimensional mechanical modeling: Journal of Geophysical Research: Solid Earth, v. 111, no. B7, p. 1–14.

Gross, M. R., 1993, The origin and spacing of cross joints: Examples from the Monterey Formation, Santa Barbara coastline, California: Journal of Structural Geology, v. 15, p. 737–751.

Gross, M. R., M. P. Fischer, T. Engelder, and R. J. Greenfield, 1995, Factors controlling joint spacing in interbedded sedimentary rocks: Integrating numerical models with field observations from the Monterey Formation, USA, *in* M. S. Ameen, ed., Fractography: Fracture topography as a tool in fracture mechanics and stress analysis: London, Geological Society, Special Publication, 92, p. 215–233.

Hagin, P. N., 1997, Joint spacing statistics in thick, homogeneous shales of the Catskill delta complex on the Appalachian Plateau: Finger Lakes region, New York, B.S. thesis, University Park, Pennsylvania State University, 138 p.

Harris, J. F., G. L. Taylor, and J. L. Walper, 1960, Relation of deformational fractures in sedimentary rocks to regional and local structure: AAPG Bulletin, v. 44, no. 12, p. 1853–1873.

Hennings, P. H., J. E. Olson, and L. B. Thompson, 2000, Combining outcrop data and three-dimensional structural models to characterize fractured reservoirs: An example from Wyoming: AAPG Bulletin, v. 84, no. 6, p. 830–849.

Hobbs, D., 1967, The formation of tension joints in sedimentary rocks: An explanation: Geological Magazine, v. 104, no. 6, p. 550–556.

Huang, Q., and J. Angelier, 1989, Fracture spacing and its relation to bed thickness: Geological Magazine, v. 126, p. 355–362.

Ji, S., and K. Saruwatari, 1998, A revised model for the relationship between joint spacing and layer thickness: Journal of Structural Geology, v. 20, no. 11, p. 1495–1508.

Ji, S., Z. Zhu, and Z. Wang, 1998, Relationship between joint spacing and bed thickness in sedimentary rocks: Effects of interbed slip: Geological Magazine, v. 135, no. 5, p. 637–655.

Lacazette, A., and T. Engelder, 1992, Fluid driven cyclic propagation of a joint in the Ithaca Siltstone, Appalachian Basin: New York, *in* B. Evans and T.-F. Wong eds., Fault Mechanics and Transport Properties of Rock: San Diego, Academic Press, p. 297–323.

Lachenbruch, A. H., 1961, Depth and spacing of tension cracks: Journal of Geophysical Research, v. 66, no. 12, p. 4273–4292.

Ladeira, F., and N. Price, 1981, Relationship between fracture spacing and bed thickness: Journal of Structural Geology, v. 3, no. 2, p. 179–183.

Lash, G., S. Loewy, and T. Engelder, 2004, Preferential jointing of Upper Devonian black shale, Appalachian Plateau, USA: Evidence supporting hydrocarbon generation as a joint-driving mechanism: London, Geological Society, Special Publication, 231, 129 p.

Lash, G. G., and T. Engelder, 2011, Thickness trends and sequence stratigraphy of the Middle Devonian Marcellus Formation, Appalachian Basin: Implications for Acadian foreland basin evolution: AAPG Bulletin, v. 95, no. 1, p. 61–103.

McLennan, J. A., P. F. Allwardt, P. H. Hennings, and H. E. Farrell, 2009, Multivariate fracture intensity prediction: Application to Oil Mountain anticline, Wyoming: AAPG Bulletin, v. 93, no. 11, p. 1585–1595.

McQuillan, H., 1973, Small-scale fracture density in Asmari Formation of southwest Iran and its relation to bed thickness and structural setting: AAPG Bulletin, v. 57, no. 12, p. 2367–2385.

Miller, T. W., 1995, New insights on natural hydraulic fractures induced by abnormally high pore pressures: AAPG Bulletin, v. 79, no. 7, p. 1005–1018.

Narr, W., and J. Suppe, 1991, Joint spacing in sedimentary rocks: Journal of Structural Geology, v. 13, no. 9, p. 1037–1048.

Nur, A., 1982, The origin of tensile fracture lineaments: Journal of Structural Geology, v. 4, no. 1, p. 31–40.

Palciauskas, V., and P. Domenico, 1980, Microfracture development in compacting sediments: Relation to hydrocarbon-maturation kinetics: AAPG Bulletin, v. 64, p. 927–937.

Pollard, D., and P. Segall, 1987, Theoretical displacements and stresses near fractures in rock: With applications to faults, joints, veins, dikes, and solution surfaces, *in* B. K. Atkinson, ed., Fracture mechanics of rock: San Diego, Academic Press, p. 277–349.

Priest, S. D., and J. A. Hudson, 1976, Discontinuity spacings in rock: International Journal of Rock Mechanics and Mining Sciences & Geomechanics Abstracts, v. 13, no. 5, p. 135–148.

Rabinovitch, A., and D. Bahat, 1999, Model of joint spacing distribution based on shadow compliance: Journal of Geophysical Research, v. 104, no. 3, p. 4877–4886.

Rives, T., M. Razack, J. P. Petit, and K. D. Rawnsley, 1992, Joint spacing: Analogue and numerical simulations: Journal of Structural Geology, v. 14, no. 8/9, p. 925–937.

Rogers, C. M., D. A. Myers, and T. Engelder, 2004, Kinematic implications of joint zones and isolated joints in the Navajo Sandstone at Zion National Park, Utah: Evidence for Cordilleran relaxation: Tectonics, v. 23, no. TC1007, p. 1–16.

Ross, S. M., 2007, Introduction to probability models: Burlington, Massachusetts, Academic Press, 800 p.

Secor, D. T., 1965, Role of fluid pressure in jointing: American Journal of Science, v. 263, p. 633.

Ungerer, P., J. Burrus, B. Doligez, P. Chenet, and F. Bessis, 1990, Basin evaluation by integrated two-dimensional modeling of heat transfer, fluid flow, hydrocarbon generation, and migration: AAPG Bulletin, v. 74, no. 3, p. 309–335.

Waters, G. A., J. R. Heinze, R. Jackson, A. A. Ketter, J. L. Daniels, and D. Bentley, 2006, Use of horizontal well image tools to optimize Barnett Shale reservoir exploitation, SPE ATCE: San Antonio, Texas, Society of Petroleum Engineers, SPE 103202, 13 p.

Wu, H., and D. D Pollard, 1995, An experimental study of the relationship between joint spacing and layer thickness: Journal of Structural Geology, v. 17, no. 6, p. 887–905.

Wu, H., and D. D. Pollard, 2002, Imaging 3-D fracture networks around boreholes: AAPG Bulletin, v. 86, no. 4, p. 593–604.